The Journal of Chemical Physics ARTICLE pubs.aip.org/aip/jcp

Diffusion and thermodiffusion of the ternary system polystyrene + toluene + cyclohexane

Cite as: J. Chem. Phys. 159, 164904 (2023); doi: 10.1063/5.0176432
Submitted: 13 September 2023 • Accepted: 9 October 2023 •
Published Online: 25 October 2023

D. Sommermann and W. Köhler[a)]

AFFILIATIONS

Physikalisches Institut, Universität Bayreuth, D-95440 Bayreuth, Germany

[a)]Author to whom correspondence should be addressed: werner.koehler@uni-bayreuth.de

ABSTRACT

We have studied diffusion and thermodiffusion in the ternary system polystyrene + toluene + cyclohexane over the entire composition range of the binary solvent toluene + cyclohexane and for polymer concentrations up to 0.1 mass fractions by multi-color optical beam deflection. The polystyrene molar masses were 4.88 and 17.90 kg/mol. The inversion problem of the contrast factor matrix could be avoided by reasonable *a priori* assumptions about the diffusion eigenvectors. The fast mode of the bimodal dynamics is attributed to the interdiffusion of the two solvents at constant polymer concentration, whereas the slow mode is due to the diffusion of the polymer with respect to the binary solvent. The amplitude of the fast mode vanishes in the pure toluene and the pure cyclohexane limits of the mixed solvent. The amplitude of the slow mode increases with polymer concentration. The composition and temperature dependence of the slow diffusion eigenvalue, the hydrodynamic correlation length, and the Soret coefficient of the polymer reflect the transition from a good to a theta solvent with increasing cyclohexane content and with decreasing temperature. Due to cross diffusion, cyclohexane reverses its migration direction between the fast and the slow mode, leading to a positive thermodiffusion but a negative Soret coefficient. The polymer thermodiffusion coefficients during the slow mode vary by approximately a factor of two, depending on the solvent composition. Rescaling with the solvent viscosity collapses all data onto a single master curve with an extrapolated value of $\eta D_T \approx 6 \times 10^{-15}$ Pa m^2 K^{-1} in the dilute limit. This value is well known from various other binary polymer/solvent mixtures.

I. INTRODUCTION

Thermodiffusion of polymers in solution has puzzled researchers since the early experiments by Debye[1] and the pioneering work performed in the group of Giddings.[2,3] One of the most surprising findings is certainly the molar mass independence of the thermophoretic mobility (thermodiffusion coefficient) of the polymer[4–15] in the dilute limit. Polymer thermodiffusion, in particular at finite concentrations, has remained an intriguing and controversial problem that touches very fundamental questions of polymer dynamics. Despite its molar mass independence, D_T is not a property of the monomer but rather of correlated units of the size of the Kuhn segment.[16–19] Surprisingly, a high molar mass plateau value of $\eta D_T \sim 6 \times 10^{-15}$ Pa m^2 K^{-1}, with η being the solvent viscosity, is common to all investigated polymers with sufficiently large Kuhn segments above ~1 kg/mol, irrespective of the solvent.[16,17] For short chains and oligomers, D_T can take almost arbitrary values, as known for small molecules, and even change its sign.

Experiments on semidilute and concentrated polymer solutions with temperature gradients are scarce.[20–23] While collective diffusion is sped up in the semidilute regime, as predicted by the blob model, thermodiffusion is not affected by chain overlap and entanglements. At high concentrations of polystyrene (PS) in toluene, a binary system with a high T_g-contrast, the glass transition is approached along the concentration axis and slows down both Fickian diffusion and thermodiffusion. Microscopic friction cancels out and does not affect the Soret coefficient, which is blind against the glass transition and nicely follows concentration scaling from the blob model.[22]

So far, thermodiffusion research on polymers has been concerned mainly with binary systems, i.e., a polymer dissolved in a pure solvent. Only few works on ternary systems exist with a polymer in a mixed solvent.[24,25] Ternary mixtures have been studied almost exclusively for small molecules, in particular in the context of the DCMIX microgravity project of ESA.[26] Their thermodiffusion behavior is significantly more diverse than the one known from binaries and unexpected findings have been reported. Singular

points inside the ternary Gibbs triangle could be identified for mixtures of water, ethanol and triethylene glycol, where all three Soret coefficients vanish simultaneously.[27] Curiously, due to cross diffusion effects, it can even occur that the thermodiffusion and the Soret coefficient have different signs.[28,29]

Measurements of the Soret effect are typically performed by means of optical techniques.[30] For ternary mixtures, traditional experiments with a single detection light source do, however, not yield sufficient information to determine the changes of the two independent composition variables. To fully analyze a ternary mixture in an optical experiment, it is necessary to measure with two different detection wavelengths and to rely on the dispersion of the refractive index to transform the results from the refractive index to the concentration space.[31,32] For this purpose, the so-called solutal contrast factor matrix needs to be inverted, which is frequently ill-conditioned and, as a consequence, greatly amplifies the experimental uncertainty.

In the following we report on measurements of polystyrene (PS) in the mixed solvent toluene (Tol) and cyclohexane (cHex) over the entire composition range of the solvent and for polymer concentrations up to $c_1 = 0.1$ (10 wt. %). We will circumvent the contrast factor matrix inversion problem by resorting to reasonable *a priori* assumptions about the directions of the eigenvectors of the diffusion matrix following a procedure developed in a previous publication.[33]

II. EXPERIMENTAL

Polystyrene (PS) polymers were obtained from PSS Polymer Standards Service GmbH with two different molar masses (PSS-ps4.5k, lot ps150410, $M_w = 4.88$ kg/mol, $M_w/M_n = 1.04$) and (PSS-ps18k, lot ps021210, $M_w = 17.90$ kg/mol, $M_w/M_n = 1.03$). The solvents were Tol (toluene, VWR AnalaR NORMAPUR, article 28 676.297, purity >99.5%) and cHex (cyclohexane, VWR AnalaR NORMAPUR, article 23 224.293, purity >99.5%). The numbering of the components is PS/Tol/cHex as $c_1/c_2/c_3$ with c_3 (cHex) as the dependent component.

The concentrations c_i are given in mass fractions. For a better distinction, we will use mass percent to indicate the composition of the binary solvent, irrespective of the polymer concentration. The ternary mass fraction is not a suitable measure for this purpose, since these numbers change also for the solvents when the polymer concentration is changed. As an example, a polymer with $c_1 = 0.1$ dissolved in a mixed solvent with composition 40:60 of Tol:cHex corresponds to concentrations $c_1/c_2/c_3 = 0.1/0.36/0.54$.

Measurements were performed by means of two different multi-color optical beam deflection (OBD) setups,[31,33–35] both equipped with interchangeable Soret cells of $h = 1.20$ mm height. The two-color OBD instrument utilizes the laser wavelengths $\lambda_1 = 405.5$ nm and $\lambda_2 = 635.0$ nm and the four-color instrument $\lambda_1 = 405.5$ nm, $\lambda_2 = 532.0$ nm, $\lambda_3 = 632.8$ nm, and $\lambda_4 = 935.0$ nm.

The solutal contrast factors $N_{c,ij} = (\partial n(\lambda_i)/\partial c_j)_{p,T,c_{k\neq j}}$ were obtained, as described in Ref. 36, from polynomial fits to refractive index measurements of concentration series in the ternary composition space as a function of the two independent concentrations c_1 and c_2. The thermal contrast factors $N_{T,ii} = (\partial n(\lambda_i)/\partial T)_{p,c_1,c_2}$ were measured interferometrically as described in Refs. 37 and 38.

III. THEORY

A. Data evaluation in refractive index space

The measurement of the Soret effect in a two-color optical beam deflection (2-OBD) experiment has been outlined in full detail in Ref. 35. The ideas how to introduce plausible *a priori* assumptions have been developed in Ref. 33. For a detailed treatment, the reader is referred to these two publications. Here, we will only reproduce a few essential equations.

The development of the concentration field in a ternary mixture subjected to a temperature gradient ∇T is described by the thermodiffusion equation in concentration space:

$$\frac{\partial \underline{c}}{\partial t} = \underline{\underline{\mathbf{D}}}(\nabla^2 \underline{c}) + \underline{D'_T}\nabla^2 T \tag{1}$$

We use the notation with an underscore for a 2d-vector in concentration space, e.g., $\underline{c} = (c_1, c_2)^T$ for the two independent concentrations and $\underline{D'_T} = (D'_{T,1}, D'_{T,2})^T$ for the corresponding primed thermodiffusion coefficients. The 2×2 diffusion matrix $\underline{\underline{\mathbf{D}}}$ has the eigenvalues $\hat{D}_1$ and $\hat{D}_2$ and the corresponding eigenvectors $\underline{v}_1$ and $\underline{v}_2$. In this work, we choose PS (c_1) and Tol (c_2) as the two independent concentrations and cHex (c_3) as the dependent one.

The signals measured in a 2-OBD experiment with the two wavelengths λ_1 and λ_2 are written, after normalization to the respective thermal amplitudes, in vector notation as

$$\underline{s}^{\mathrm{norm}}(t) = \underline{1} + \underline{\underline{\mathbf{M}}}\,\underline{f}(t), \tag{2}$$

The vector $\underline{f}(t) = (f(\hat{D}_1, t), f(\hat{D}_2, t))^T$ contains the normalized functions $f(\hat{D}_i, t)$ that describe the bimodal build-up of the concentration gradient.[35] A simultaneous fit of Eq. (2) to the two-color signals yields six unknown parameters: the two diffusion eigenvalues $\hat{D}_i$ and the four entries M_{ij} of the amplitude matrix.

B. The standard ternary method

For the transformation from refractive index to concentration space, the thermal and solutal contrast factor matrices $\underline{\underline{\mathbf{N_T}}}$ [with $N_{T,ij} = (\partial n_i/\partial T)_{c_1,c_2,p}\,\delta_{ij}$] and $\underline{\underline{\mathbf{N_c}}}$ [with $N_{c,ij} = (\partial n_i/\partial c_j)_{c_{k\neq j},T,p}$] are required. They are either measured in separate experiments or calculated from suitable model equations.[39] Finally, the thermodiffusion coefficients $\underline{D'_T}$, the Soret coefficients $\underline{S'_T}$ of the two independent concentrations and the diffusion matrix $\underline{\underline{\mathbf{D}}}$ are obtained as

$$\underline{\underline{\mathbf{D}}} = (\underline{\underline{\mathbf{N_c}}}^{-1}\,\underline{\underline{\mathbf{N_T}}}\,\underline{\underline{\mathbf{M}}})\,\underline{\underline{\hat{\mathbf{D}}}}\,(\underline{\underline{\mathbf{M}}}^{-1}\,\underline{\underline{\mathbf{N_T}}}^{-1}\,\underline{\underline{\mathbf{N_c}}}) \tag{3}$$

$$\underline{D'_T} = -\underline{\underline{\mathbf{N_c}}}^{-1}\,\underline{\underline{\mathbf{N_T}}}\,\underline{\underline{\mathbf{M}}}\,\underline{\underline{\hat{\mathbf{D}}}}\,\underline{1} \tag{4}$$

$$\underline{S'_T} = -\underline{\underline{\mathbf{N_c}}}^{-1}\,\underline{\underline{\mathbf{N_T}}}\,\underline{\underline{\mathbf{M}}}\,\underline{1}. \tag{5}$$

As can be seen from Eq. (5), only the two asymptotic steady state amplitudes $M_{i1} + M_{i2}$ $(i = 1, 2)$ are required for the Soret coefficients, without the need to resolve the bimodal time dependencies.

Different two-color optical experiments performed in different laboratories, including the DCMIX microgravity experiments,[26]

are evaluated by variations of this approach with fitting in different parameter spaces.[40] Nevertheless, all these procedures rely on the transformation to the composition space by means of the solutal contrast factor matrix and are more or less equivalent. Also thermogravitational column experiments,[41] with measurement of refractive index and density changes, fall into the same category. The fundamental problem of this approach, which we may call the standard ternary evaluation method, is the need to invert the frequently ill-conditioned solutal contrast factor matrix $\underline{\underline{\mathbf{N}}}_c$.[42]

C. Fixing the diffusion eigenvectors

In Ref. 33 we have shown that the unfavorable error amplification of the standard ternary evaluation can drastically be reduced by reasonable *a priori* assumptions about the directions of the diffusion eigenvectors.

Figure 1 shows the solutal part of the beam deflection signal as measured with the blue laser wavelength together with fits according to Eq. (2). In the upper part, the normalized signals are shown for different polymer concentrations in the same mixed solvent with equal mass fractions of Tol and cHex. A slow mode, whose amplitude increases with polymer concentration, and a shallow dip at short times are clearly discernible.

In the lower part of Fig. 1, the curve for a polymer concentration $c_1 = 0.04$ is analyzed in detail. The fit reveals a distinct bimodal time dependence, corresponding to the two diffusion eigenvalues. In general, the diffusion modes have no simple ad-hoc interpretation in a ternary system with small molecules. In the case of large polymer molecules in a mixed solvent, however, our assumption is that the fast mode can be attributed to the interdiffusion of the two solvents at constant polymer concentration, whereas the slow mode reflects the polymer diffusion with respect to the mixed solvent of constant composition. While this assumption is plausible, it needs further justification, which was given in Ref. 33 during the discussion of the results.

Additional arguments can be derived from a closer inspection of the fast and the slow mode extracted from the bimodal fit in Fig. 1 (bottom). For comparison, the signals from related binary mixtures, namely the Tol/cHex mixture without polymer and the polymer in the two pure solvents (PS/Tol and PS/cHex) are included in the graph. The fast mode is very close to the signal from Tol/cHex: both have a negative sign, similar amplitudes and almost identical time constants. Correspondingly, the slow mode and the two binary polymer solutions (PS/Tol and PS/cHex) share the positive amplitude and similar time constants. Even more, the amplitudes of the polymer in the two pure solvents bracket the amplitude of the slow mode in the mixed solvent.

The assignment of the two diffusion modes fixes the normalized diffusion eigenvectors in the space of the independent concentrations c_1 (PS) and c_2 (Tol) to[33]

$$\underline{v}_1 = \begin{pmatrix} 0 \\ 1 \end{pmatrix}, \quad \underline{v}_2 = \frac{1}{\sqrt{1+(1+r)^2}} \begin{pmatrix} 1+r \\ -1 \end{pmatrix}. \tag{6}$$

Here, $r = c_3/c_2$ is the composition ratio of the mixed solvent. The diffusion matrix $\underline{\underline{\mathbf{D}}}$ in the (c_1, c_2)-space is obtained from the diagonal

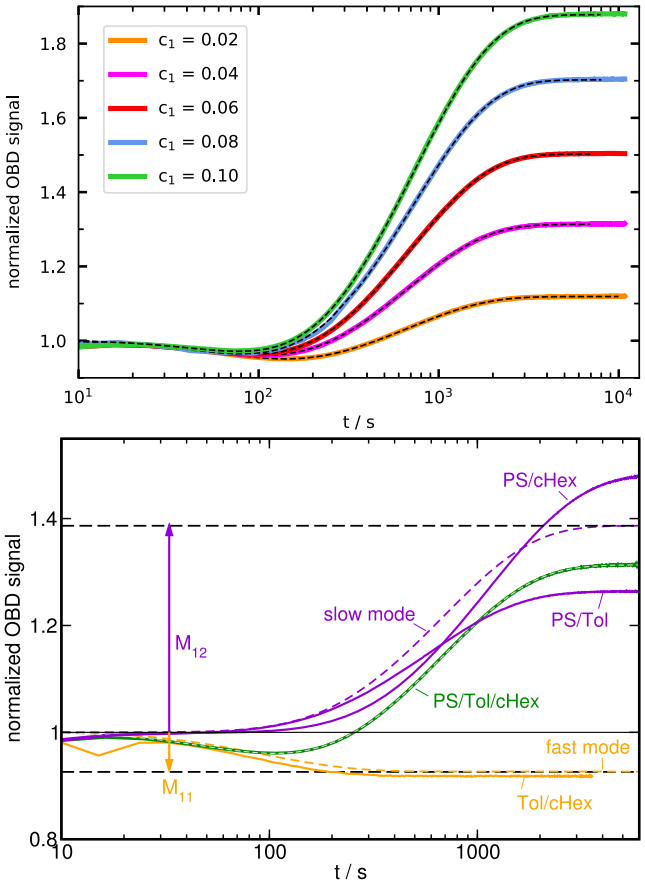

FIG. 1. Top: solutal part of the normalized OBD signal for a symmetric binary solvent with equal mass fractions of Tol and cHex. The polymer concentration varies between 0.02 and 0.1. The dashed lines are fits of Eq. (2). Bottom: detailed analysis of measurement with polymer concentration $c_1 = 0.04$. The dashed lines show the fit curve and separately the slow and the fast mode. For comparison the solutal signals for the binary solvent (Tol/cHex) and for the polymer in the two pure solvents (PS/Tol and PS/cHex) are also plotted. The early data points around 20–30 s still show some influence from the temperature switching and have been excluded from the fit. Wavelength $\lambda_1 = 405.5$ nm, $\delta = 25\,^{\circ}$C. Polymer molar mass $M_w = 4.88$ kg/mol.

diffusion matrix $\hat{\underline{\underline{\mathbf{D}}}}$ according to $\underline{\underline{\mathbf{D}}} = \underline{\underline{\mathbf{V}}}\,\hat{\underline{\underline{\mathbf{D}}}}\,\underline{\underline{\mathbf{V}}}^{-1}$, where the transformation matrix $\underline{\underline{\mathbf{V}}} = (\underline{v}_1, \underline{v}_2)$ contains the eigenvectors as column vectors.

Once the diffusion eigenvectors are set, the asymptotic steady state concentration change $\delta C_{\infty,j}$ in the directions of the eigenvector v_j is obtained from the measurement with a *single wavelength* λ_i:

$$\delta C_{\infty,j} = \frac{M_{ij}\,\delta T}{V_{1j}N_{c,i1}/N_{T,ii} + V_{2j}N_{c,i2}/N_{T,ii}} \tag{7}$$

Contrary to the six fit parameters obtained from a two-color measurement, a single-color experiment yields only four of them: the two amplitudes $M_{i,1}$ and $M_{i,2}$ and the two diffusion eigenvalues $\hat{D}_1$ and $\hat{D}_2$.

The concentration changes $\delta C_{\infty,j}$ can be projected onto the c_1- and the c_2-axes. Since the index $j = 1$ corresponds to the fast and $j = 2$ to the slow mode, the partial primed Soret coefficients for the two modes and the total primed Soret coefficient of the asymptotic steady state of the entire ternary system are

$$\underline{S_T}'^{\,\text{fast}} = -\frac{1}{\delta T}\,\delta\underline{c}^{\,\text{fast}} = -\frac{\delta C_{\infty,1}}{\delta T}\begin{pmatrix} V_{11} \\ V_{21} \end{pmatrix} \tag{8}$$

$$\underline{S_T}'^{\,\text{slow}} = -\frac{1}{\delta T}\,\delta\underline{c}^{\,\text{slow}} = -\frac{\delta C_{\infty,2}}{\delta T}\begin{pmatrix} V_{12} \\ V_{22} \end{pmatrix} \tag{9}$$

$$\underline{S_T}' = \underline{S_T}'^{\,\text{fast}} + \underline{S_T}'^{\,\text{slow}} = -\frac{1}{\delta T}\,\underline{\underline{\mathbf{V}}}\,\underline{\delta C_\infty}. \tag{10}$$

The corresponding primed thermodiffusion coefficients are

$$\underline{D_T}'^{\,\text{fast}} = \hat{D}_1\,\underline{S_T}'^{\,\text{fast}} \tag{11}$$

$$\underline{D_T}'^{\,\text{slow}} = \hat{D}_2\,\underline{S_T}'^{\,\text{slow}} \tag{12}$$

$$\underline{D_T}' = \underline{\underline{\mathbf{D}}}\,\underline{S_T}' = \begin{pmatrix} \hat{D}_2 & 0 \\ \dfrac{\hat{D}_1 - \hat{D}_2}{1+r} & \hat{D}_1 \end{pmatrix}\underline{S_T}'. \tag{13}$$

Since the entire process is a ternary one, whereas the fast and the slow process are effectively binary in nature, there exist several relations between the Soret and between the thermodiffusion coefficients of the three components.

As always, the sum of all three coefficients is zero, which holds in any case due to mass conservation:

$$\sum_{i=1}^{3} S'^{\text{fast}}_{T,i} = \sum_{i=1}^{3} S'^{\text{slow}}_{T,i} = \sum_{i=1}^{3} S'_{T,i} = 0 \tag{14}$$

$$\sum_{i=1}^{3} D'^{\text{fast}}_{T,i} = \sum_{i=1}^{3} D'^{\text{slow}}_{T,i} = \sum_{i=1}^{3} D'_{T,i} = 0 \tag{15}$$

Besides that, there are some additional relations that follow from the directions of the diffusion eigenvectors:

$$S'^{\text{fast}}_{T,3} = -S'^{\text{fast}}_{T,2} \tag{16}$$

$$S'^{\text{fast}}_{T,1} = 0 \tag{17}$$

$$S'^{\text{slow}}_{T,3} = r\,S'^{\text{slow}}_{T,2} \tag{18}$$

$$S'^{\text{slow}}_{T,1} = -S'^{\text{slow}}_{T,2}(1+r) \tag{19}$$

Finally, effective binary Soret coefficients (without "prime") are defined for the two modes by introducing suitable concentration prefactors:[33]

$$S^{\text{fast}}_{T,i} = \frac{1}{c_2 c_3}\,S'^{\text{fast}}_{T,i} \qquad (i = 2, 3) \tag{20}$$

$$S^{\text{slow}}_{T,1} = \frac{1}{c_1(c_2+c_3)}\,S'^{\text{slow}}_{T,1} \tag{21}$$

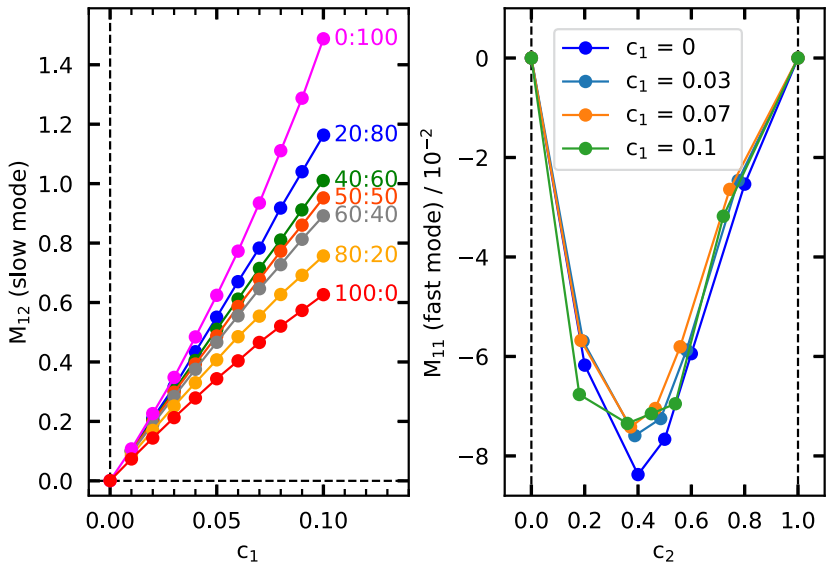

FIG. 2. Left: amplitude M_{12} of the slow mode as a function of PS concentration c_1 for different solvent compositions Tol:cHex in percent. Right: amplitude M_{11} of the fast mode as a function of Tol concentration c_2 for different polymer concentrations c_1. Temperature $\theta = 20\,^{\circ}\text{C}$. Polymer molar mass $M_w = 4.88$ kg/mol.

Relations equivalent to Eqs. (16)–(21) hold also for the thermodiffusion coefficients. Suitable concentration prefactors for the definition of transformation invariant Soret and thermodiffusion coefficients of the entire ternary process have been developed by Ortiz de Zárate[43] and have been employed for the case of a polymer in a mixed solvent in Ref. 33.

IV. RESULTS AND DISCUSSION

Measurements have been performed at four different temperatures (20, 25, 30, and 35 °C) over the entire composition range of the binary solvent and for polymer concentrations ranging from $c_1 = 0$ to $c_1 = 0.1$ in steps of $\delta c_1 = 0.01$. The evaluation of the raw data was performed as explained in Fig. 1.

The amplitudes of the two modes are plotted in Fig. 2 as a function of polymer concentration and solvent composition, which clearly supports our mode assignment. The slow mode vanishes for vanishing polymer concentration, whereas the fast mode vanishes in the two binary limits of the neat solvents. Furthermore, the amplitude of the fast mode neither depends on the concentration (Fig. 2 right) nor on the molar mass (not shown) of the polymer.

A. Diffusion coefficients

Figure 3 presents the two diffusion eigenvalues for the fast and the slow mode of both polymer molar masses, measured at a temperature of $\theta = 20$ °C. The measurements at the other temperatures show somewhat shifted values but generally the same picture.

The fast mode ($\hat{D}_1$) shows a significantly larger scatter, which is owed to the small amplitude of this mode, in particular for asymmetric solvent compositions. Its separation from the much stronger slow mode becomes more difficult with increasing polymer concentration due to the increasing amplitude of the latter. The first points, at $c_1 = 0$, are the diffusion coefficients measured for the binary Tol/cHex mixtures. Within the, admittedly significant, noise level, there is neither a systematic influence of the polymer concentration nor of the molar mass. Furthermore, $\hat{D}_1$ is identical to the diffusion coefficient of the binary solvent mixture of the corresponding composition, in agreement with our initial assignment of the two modes. There is also a good agreement with a literature value for the diffusion coefficient of the binary solvent of symmetric composition, where $D = 1.79 \times 10^{-9}$ m^2/s at $\theta = 25$ °C has been reported in Ref. 44 as compared to $D_1 = 1.67 \times 10^{-9}$ m^2/s at $\theta = 20$ °C in our experiments for the same mixture.

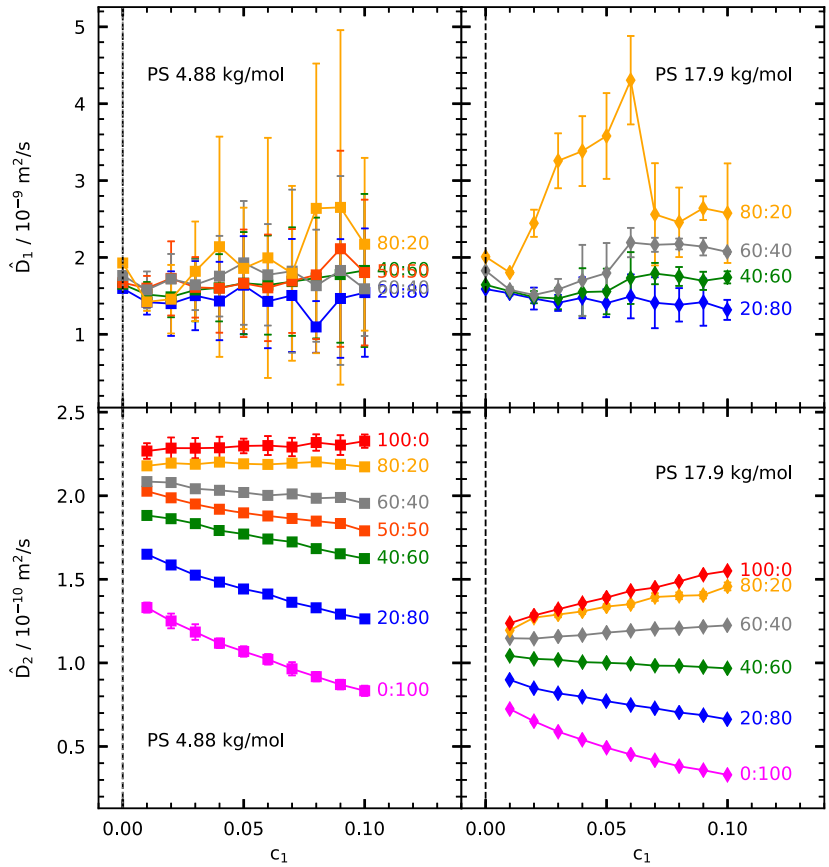

FIG. 3. Diffusion eigenvalues $\hat{D}_1$ (top row) and $\hat{D}_2$ (bottom row) for PS of 4.88 kg/mol (left column) and 17.90 kg/mol (right column) as function of PS concentration c_1 in different solvent compositions (Tol:cHex in percent). Temperature $\theta = 20$ °C. The values for $c_1 = 0$ in the upper row are the diffusion coefficients of the binary solvent mixtures.

Due to the larger amplitude of the slow mode, there is much less noise on the $\hat{D}_2$ values, which show a distinctly different pattern from the faster eigenvalue $\hat{D}_1$. The slope of $\hat{D}_2(c_1)$ monotonously changes from positive in the good solvent toluene to negative in the theta solvent cyclohexane. The effect is more pronounced for the longer chain length.

Since the diffusion coefficient depends on both a frictional and a thermodynamic contribution, it is advantageous to factor out the influence of the viscosity, which is responsible for the vertical shift of the different $\hat{D}_2$ values in the limit of vanishing polymer concentration. A suitable quantity is the hydrodynamic screening length[45–47]

$$\xi_h = \frac{k_B T}{6\pi\eta_0 D_c}, \tag{22}$$

where k_B and η_0 are Boltzmann's constant and the solvent viscosity, respectively. In the limit of infinite dilution, ξ_h becomes identical to the hydrodynamic radius of a single coil. Based on our assumptions, the cooperative diffusion coefficient D_c is equal to $\hat{D}_2$.

Figure 4 shows ξ_h as obtained from the $\hat{D}_2$ values in Fig. 3. The hydrodynamic radii in the infinite dilution limit are practically identical for every solvent composition. Only for pure cyclohexane (0:100) the value is somewhat lower. This effect might be caused by a slight shrinkage of the polymer coil due to the poorer solvent quality, but it is not very pronounced and barely exceeds the error level due to the relatively short polymer chains investigated. The slopes $d\xi_h/dc_1(c_1 = 0)$ from the upper row in Fig. 4 are plotted in the lower row as a function of the cHex concentration for the four investigated temperatures.

The steep increase of the hydrodynamic correlation length with increasing cyclohexane content and polymer concentration, in particular for the longer chains, reflects the approach to the coexistence line and the spinodal. The phase diagram of PS/cHex shows a lower miscibility gap and a theta temperature of 307.25 K (34.1 °C) for infinite chain length and vanishing polymer concentration.[48] The coexistence curve shifts towards lower temperatures and higher polymer concentrations with decreasing chain length of the polymer.[49–51]

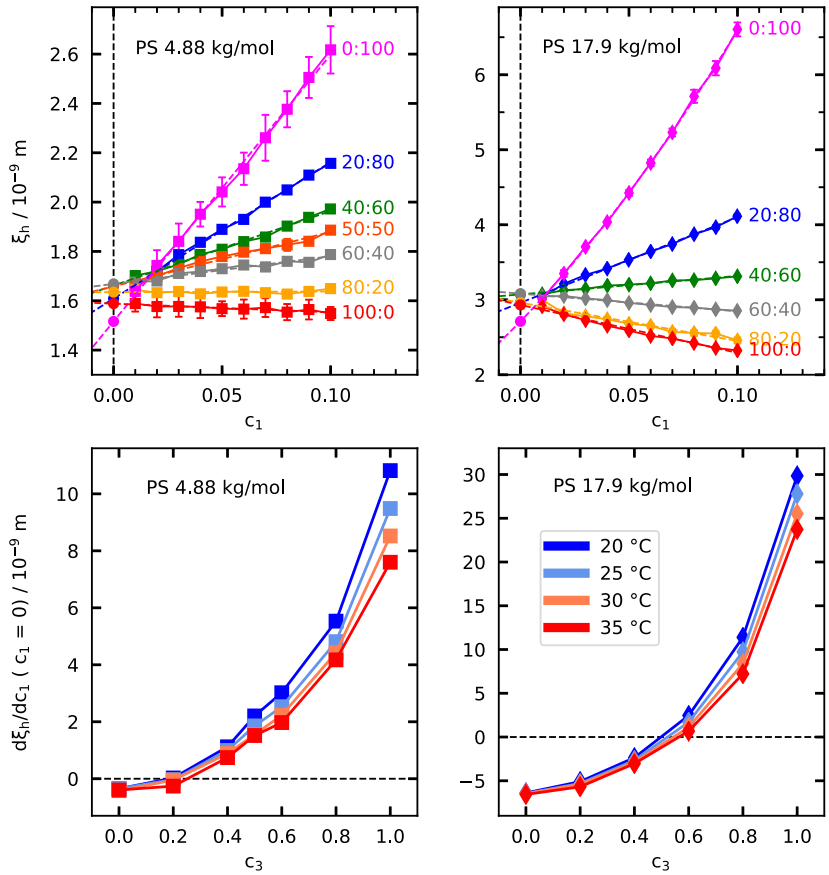

FIG. 4. Top: Hydrodynamic correlation length ξ_h for PS of 4.88 kg/mol (top left) and 17.90 kg/mol (top right) as function of PS concentration c_1 in different solvent compositions (Tol:cHex in percent). Temperature $\theta = 20\,°C$. Bottom: slopes of $\xi_h(c_1)$ from plots in top row plotted as a function of the cyclohexane content c_3 of the binary solvent for different temperatures.

Siporska *et al.* have determined the coexistence curves of PS in cyclohexane for molar masses between 25 and 13 200 kg/mol.[52] They have provided a parametrization $\varphi_c(M_w) = 7.16 \times M_w^{-0.38}$ for the critical volume fraction and $1/T_c = a + b/\sqrt{M_w}$ for the critical temperature. The parameters $a = 0.003\,26$ and $b = 0.0478$ are not given in Ref. 52 but have been calculated from a fit to the reported data. By extrapolating to lower molar masses, and converting from volume to mass fractions by $c_1 = \varphi_1\rho_1/(\varphi_1\rho_1 + \varphi_3\rho_3)$ with $\rho_1 = 1050$ kg/m^3 and $\rho_3 = 780$ kg/m^3, the critical points for our PS/cHex solution are obtained as ($\varphi_c = 0.284$, $c_c = 0.348$, $T_c = 253.25$ K) for $M_w = 4.88$ kg/mol and ($\varphi_c = 0.173$, $c_c = 0.219$, $T_c = 276.16$ K) for $M_w = 17.90$ kg/mol. Thus, both of our samples are always in the homogeneous state above the coexistence curve. Both an increase of the polymer concentration and a lowering of the temperature, as well as a higher cHex content brings them closer to the critical point and the spinodal, which is reflected by a slowing down of diffusion[53,54] and the increasing correlation length ξ_h in Fig. 4.

B. Soret and thermodiffusion coefficients

The scenario concerning the Soret and the thermodiffusion coefficients in this ternary system is very rich and space does not permit to discuss all aspects in detail. In the following we will focus on some very characteristic and sometimes also surprising results without any attempt for completeness. For illustration, some Soret coefficients are shown in Fig. 5 for the fast mode ($S'^{\text{fast}}_{T,3}$), the slow mode ($S'^{\text{slow}}_{T,3}$) and the total Soret coefficient of cHex ($S'_{T,3}$) and for the slow mode of PS ($S'^{\text{slow}}_{T,1}$). The steep increase of the modulus of $S'^{\text{slow}}_{T,1}$ with increasing cHex content reflects the approach to the coexistence curve and the spinodal in the same way as the increasing hydrodynamic correlation length in Fig. 4.

1. The signs of the Soret and thermodiffusion coefficients

The generic behaviour of the primed Soret and thermodiffusion coefficients in the case of finite concentrations of all three components is the following:

Fast mode: the polymer does not participate in the fast mode, during which cyclohexane moves to the cold and toluene to the hot, irrespective of polymer concentration. Hence, $S'^{\text{fast}}_{T,1} = D'^{\text{fast}}_{T,1} = 0$, both $S'^{\text{fast}}_{T,2}$ and $D'^{\text{fast}}_{T,2}$ are negative, both $S'^{\text{fast}}_{T,3}$ and $D'^{\text{fast}}_{T,3}$ are positive. The values of all coefficients are close to their values in the corresponding binary solvent mixtures without polymer.

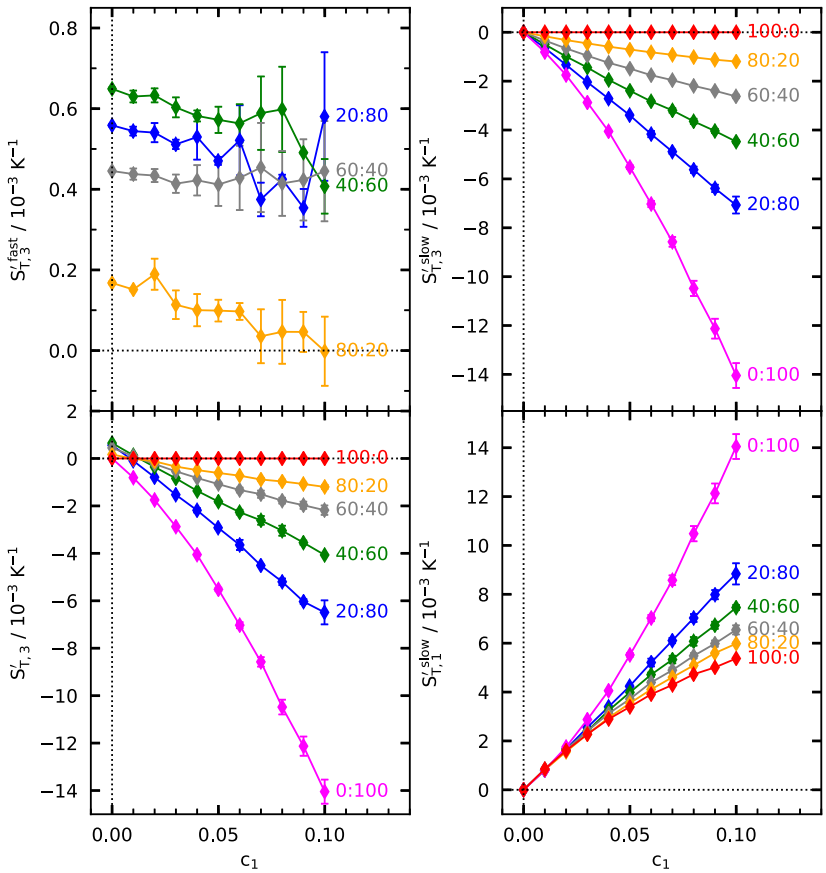

FIG. 5. Selected primed Soret coefficients of PS and cHex. Fast mode ($S'^{\text{fast}}_{T,3}$) (top left), slow mode ($S'^{\text{slow}}_{T,3}$) (top right) and total Soret coefficient of cHex ($S'_{T,3}$) (bottom left). Slow mode of PS ($S'^{\text{slow}}_{T,1}$) (bottom right). Solvent compositions (Tol:cHex in percent), PS ($M_w = 17.90$ kg/mol), Temperature $\theta = 20$ °C.

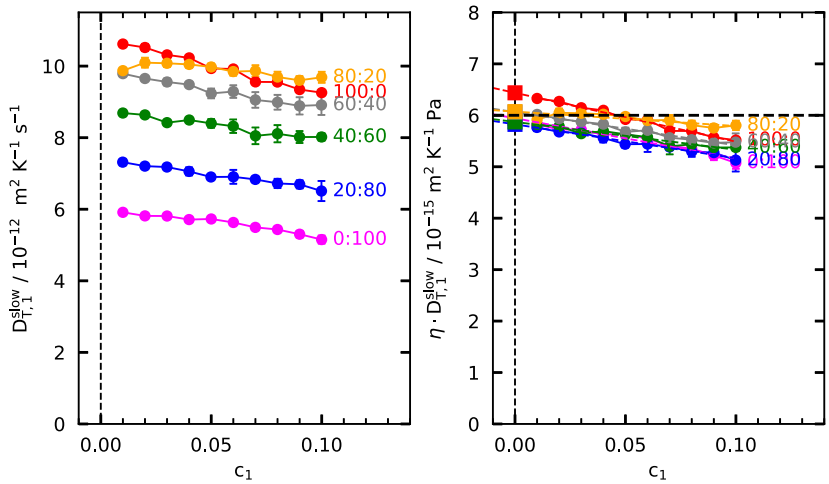

FIG. 6. Thermodiffusion coefficient of PS for the slow mode, $D_{T,1}^{slow}$ (left), and the viscosity-scaled value $\eta D_{T,1}^{slow}$ (right). The dashed horizontal line in the right plot marks the universal value $\eta D_T \approx 6 \times 10^{-15}$ Pa m^2 K^{-1}. Solvent compositions (Tol:cHex in percent), PS (M_w = 17.90 kg/mol), Temperature θ = 20 °C.

Slow mode: the polymer migrates to the cold, the mixed solvent, whose composition does not change during the slow mode, to the hot. Hence, both $S_{T,1}^{\prime slow}$ and $D_{T,1}^{\prime slow}$ are positive, whereas $S_{T,2}^{\prime slow}$, $D_{T,2}^{\prime slow}$, $S_{T,3}^{\prime slow}$, and $D_{T,3}^{\prime slow}$ are all negative.

Total: The total primed Soret and thermodiffusion coefficients are the respective sums over the slow and the fast mode. Since the fast mode does not contribute to the polymer thermodiffusion, it follows immediately from the slow mode that both $S_{T,1}^{\prime}$ and $D_{T,1}^{\prime}$ are positive. Since Tol migrates to the hot, both with respect to cHex during the fast mode and with respect to PS during the slow mode, $S_{T,2}^{\prime}$ and $D_{T,2}^{\prime}$ are negative. A peculiar situation arises for cHex, which migrates to the cold during the fast and to the hot during the slow mode. This causes a sign change of $S_{T,3}^{\prime}$, which is positive for very small polymer concentrations around $c_1 \sim 0.01$ and negative above (Fig. 5 bottom left). Surprising are the different signs of the thermodiffusion and the Soret coefficient of cHex. The sign of $S_{T,3}^{\prime}$ is negative whereas $D_{T,3}^{\prime}$ is positive for all solvent compositions and all polymer concentrations above $c_1 \sim 0.01$.

Different signs of the thermodiffusion and the Soret coefficient are not possible in a binary mixture, which is also why the signs of both coefficients always agree within the fast and within the slow mode. The situation is different for ternary mixtures, where different signs of the two coefficients have already been reported for the system toluene/methanol/cyclohexane.[28,29] The thermodiffusion coefficient is a measure for the thermophoretic velocity in the homogeneous initial state, whereas the Soret coefficient determines the separation in the asymptotic nonequilibrium steady state. In our case, this means that cyclohexane first migrates towards the cold, corresponding to the positive $D_{T,3}^{\prime fast}$, and then changes its migration direction towards the hot during the slow mode. This reversal of the direction is a direct consequence of the cross diffusion coefficient D_{21} in the diffusion matrix in Eq. (13).

2. The universal thermophoretic velocity

Next, we want to test the universality of the thermophoretic mobility, as reported in the literature[16,17] for binary polymer solutions, for the case of the here discussed ternary mixtures. The finding for the binaries was that the variation of the thermodiffusion coefficient between solutions of different polymers in different solvents is essentially a viscosity effect. The only requirement is, that the polymers are sufficiently stiff with Kuhn segments of at least say 1 kg/mol. PS falls into this category, where a universal value of the product of the solvent viscosity η with the thermodiffusion coefficient D_T in the dilute limit assumes a universal value of $\eta D_T \approx 6 \times 10^{-15}$ Pa m^2 K^{-1}. Surprisingly, this value depends neither on the solvent nor on the polymer type or molar mass.

In order to test this finding, it is necessary to consider the effective binary thermodiffusion coefficient (without prime) that includes the proper concentration prefactor and that relates only to the motion of the polymer with respect to the mixed solvent. According to our model, this is $D_{T,1}^{slow} = [c_1(c_2 + c_3)]^{-1} D_{T,1}^{\prime slow}$ defined in analogy to Eq. (21). The viscosities of the Tol/cHex solvent mixture were calculated as described in Refs. 33 and 55.

Figure 6 shows the plots of $D_{T,1}^{slow}$ and of $\eta D_{T,1}^{slow}$ as a function of the PS concentration c_1 for the different solvent compositions. For all mixtures, the dilute limits of $\eta D_{T,1}^{slow}$ collapse towards the universal value of $\approx 0.6 \times 10^{-14}$ Pa m^2 K^{-1}, confirming the universality also for the polymers in mixed solvents. Shown is only the result for M_w = 17.90 kg/mol at θ = 20 °C, but the results are almost identical for the smaller molar mass and for all temperatures.

V. SUMMARY AND CONCLUSION

We have investigated diffusion and thermodiffusion of polystyrene up to a mass fraction of $c_1 = 0.1$ in the mixed solvent toluene + cyclohexane over its entire composition space. The OBD signals are distinctly bimodal. The fast mode can be attributed to the interdiffusion of the solvent. Its amplitude vanishes in the two limiting cases of pure toluene and pure cyclohexane. The associated diffusion eigenvalues $\hat{D}_1$ agree well with the diffusion coefficients of the respective binary Tol/cHex-mixtures and are not sensitive to the polymer concentration. The latter observation is in contradiction to

light scattering experiments of Negadi *et al.*, who observed a significant decrease of the amplitude of the fast mode with increasing polymer concentration.[56]

The slow mode is attributed to the diffusion of the polymer with respect to the mixed solvent. The small diffusion eigenvalues $\hat{D}_2$ are identical to the polymer diffusion coefficients. The hydrodynamic correlation length calculated therefrom shows a distinct dependence on the solvent quality. It increases with increasing cyclohexane content and, hence, decreasing solvent quality. Under all experimental conditions our system was in the homogeneous miscible state above the coexistence curve. Both an increase of the cyclohexane content in the binary solvent, a decrease of the temperature and an increase of the polymer concentration bring the system closer to the coexistence line and the spinodal, which leads to a slowing down of diffusion, an increase of the hydrodynamic correlation length and an increase of the Soret coefficient.

Due to cross diffusion terms between the polymer and the two solvents, a peculiar situation arises, where the thermodiffusion and the Soret coefficient of cyclohexane do not have the same sign. While this is not possible in binary mixtures, it can occur in ternaries and indicates a reversal of the migration direction of cyclohexane during the development of the nonequilibrium steady state out of the initial homogeneous equilibrium state.

The interpretation of the slow mode as an essentially binary process with a fixed solvent composition allowed to compare the ternary mixture to solutions of polymers in pure solvents, i.e., binary mixtures. For these systems it has been found that the thermodiffusion coefficient is predominantly controlled by the solvent viscosity, provided the Kuhn segments are significantly, i.e., one order of magnitude, larger than the solvent molecules. We have been able to show that the same universality holds in the investigated ternary systems for the product of the thermodiffusion coefficient of the polymer and the viscosity of the mixed solvent.

All data evaluation was based on the assignment of the fast and the slow mode to the solvent and the polymer process. This fixes the directions of the diffusion eigenvectors in concentration space and allows to circumvent the error-prone inversion of the solutal contrast factor matrix otherwise unavoidable in optical experiments on ternary mixtures. As a result, the accuracy is tremendously improved with errors not significantly larger than for binary mixtures. While there is no unequivocal proof that this interpretation is correct, the resulting picture is very consistent with smooth transitions to the binary boundaries in the ternary composition diagram.

The ideas developed in this work and in Ref. 33 are not limited to OBD experiments but are also applicable to other techniques, e.g., optical digital interferometry, the Selectable Optical Diagnostics Instrument (SODI) aboard the International Space Station, thermal diffusion forced Rayleigh scattering, thermogravitational columns, or shadowgraphy of non-equilibrium fluctuations. A recent review of these techniques can be found in Ref. 30. Besides polymers, also colloids in mixed solvents are possible candidates for the here developed procedure. In any case, a clear separation and assignment of the diffusion eigenvalues is a necessary prerequisite. Both is generally not possible in ternary mixtures of small molecules with similar diffusion eigenvalues. For these, the inversion of the contrast factor matrix appears unavoidable.

ACKNOWLEDGMENTS

This work was supported by Deutsches Zentrum für Luft- und Raumfahrt (DLR, Grant No. 50WM2147) and by Deutsche Forschungsgemeinschaft (DFG, Grant No. DFG, KO1541/13-1).

AUTHOR DECLARATIONS

Conflict of Interest

The authors have no conflicts to disclose.

Author Contributions

D. Sommermann: Conceptualization (equal); Data curation (lead); Formal analysis (equal); Investigation (lead); Software (lead); Writing – original draft (equal); Writing – review & editing (equal). **W. Köhler**: Conceptualization (equal); Formal analysis (equal); Funding acquisition (lead); Investigation (supporting); Project administration (lead); Supervision (lead); Writing – original draft (equal); Writing – review & editing (equal).

DATA AVAILABILITY

The data that support the findings of this study are available from the corresponding author upon reasonable request.

REFERENCES

[1] P. Debye and A. M. Bueche, in *High-Polymer Physics*, edited by H. A. Robinson (Remsen Press Division, Brooklyn, 1948), p. 497.
[2] J. C. Giddings, K. D. Caldwell, and M. N. Myers, Macromolecules **9**, 106 (1976).
[3] M. E. Schimpf and J. C. Giddings, J. Polym. Sci., Part B: Polym. Phys. **27**, 1317 (1989).
[4] E. P. C. Mes, W. T. Kok, and R. Tijssen, Int. J. Polym. Anal. Charact. **8**, 133 (2003).
[5] F. Brochard and P.-G. de Gennes, C. R. Acad. Sc. Paris, Ser. 2 **293**, 1025 (1981).
[6] S. Semenov and M. Schimpf, Phys. Rev. E **69**, 011201 (2004).
[7] A. Würger, Phys. Rev. Lett. **98**, 138301 (2007).
[8] E. Bringuier, C. R. Mec. **339**, 349 (2011).
[9] E. Bringuier, Physica A **389**, 4545 (2010).
[10] M. E. Schimpf and S. N. Semenov, Philos. Mag. **83**, 2185 (2003).
[11] M. E. Schimpf and J. C. Giddings, J. Polym. Sci., Part B: Polym. Phys. **28**, 2673 (1990).
[12] R. Kita and S. Wiegand, Macromolecules **38**, 4554 (2005).
[13] S. Wongsuwarn *et al.*, Soft Matter **8**, 5857 (2012).
[14] A. Königer *et al.*, Soft Matter **9**, 1418 (2013).
[15] K. I. Morozov and W. Köhler, Langmuir **30**, 6571 (2014).
[16] D. Stadelmaier and W. Köhler, Macromolecules **41**, 6205 (2008).
[17] D. Stadelmaier and W. Köhler, Macromolecules **42**, 9147 (2009).
[18] J. Rauch and W. Köhler, Macromolecules **38**, 3571 (2005).
[19] A. Würger, Phys. Rev. Lett. **102**, 078302 (2009).
[20] F. Schwaiger and W. Köhler, Macromolecules **46**, 1673 (2013).
[21] J. Rauch and W. Köhler, Phys. Rev. Lett. **88**, 185901 (2002).
[22] J. Rauch and W. Köhler, J. Chem. Phys. **119**, 11977 (2003).
[23] K. J. Zhang *et al.*, J. Chem. Phys. **111**, 2270 (1999).
[24] B. J. de Gans, R. Kita, S. Wiegand, and J. Luettmer-Strathmann, Phys. Rev. Lett. **91**, 245501 (2003).
[25] L. García-Fernández *et al.*, Eur. Phys. J. E **42**, 124 (2019).
[26] M. Braibanti *et al.*, Eur. Phys. J. E **42**, 86 (2019).

[27]M. Schraml, H. Bataller, C. Bauer *et al.*, Eur. Phys. J. E **44**, 128 (2021).
[28]B. Seta *et al.*, Phys. Fluids **35**, 021702 (2023).
[29]B. Seta, A. Errarte, A. Mialdun *et al.*, Phys. Chem. Chem. Phys. **25**, 15715 (2023).
[30]W. Köhler, A. Mialdun, M. M. Bou-Ali, and V. Shevtsova, Int. J. Thermophys. **44**, 140 (2023).
[31]K. B. Haugen and A. Firoozabadi, J. Phys. Chem. B **110**, 17678 (2006).
[32]V. Shevtsova, V. Sechenyh, A. Nepomnyashchy, and J. C. Legros, Philos. Mag. **91**, 3498 (2011).
[33]D. Sommermann, M. Schraml, and W. Köhler, J. Chem. Phys. **157**, 194903 (2022).
[34]A. Königer, H. Wunderlich, and W. Köhler, J. Chem. Phys. **132**, 174506 (2010).
[35]M. Gebhardt and W. Köhler, J. Chem. Phys. **142**, 084506 (2015).
[36]M. Gebhardt and W. Köhler, Eur. Phys. J. E **38**, 24 (2015).
[37]G. Wittko and W. Köhler, Philos. Mag. **83**, 1973 (2003).
[38]A. Königer, B. Meier, and W. Köhler, Philos. Mag. **89**, 907 (2009).
[39]M. Gebhardt *et al.*, J. Chem. Phys. **138**, 114503 (2013).
[40]A. Mialdun *et al.*, J. Chem. Phys. **148**, 044506 (2018).
[41]M. Larrañaga *et al.*, J. Chem. Phys. **143**, 024202 (2015).
[42]T. Triller, D. Sommermann, M. Schraml *et al.*, Eur. Phys. J. E **42**, 27 (2019).
[43]J. M. Ortiz de Zárate, Eur. Phys. J. E **42**, 43 (2019).
[44]G. Wittko, "Uber den Einfluss molekularer Parameter auf die Transporteigenschaften organischer Lösungsmittel," Ph.D. thesis, University of Bayreuth, 2007.
[45]A. Bennett, P. Daivis, R. Shanks, and R. Knott, Polymer **45**, 8531 (2004).
[46]F. Brochard and P. G. de Gennes, Macromolecules **10**, 1157 (1977).
[47]P. G. De Gennes, Macromolecules **9**, 594 (1976).
[48]J. Hager, M. Anisimov, J. Sengers, and E. E. Gorodetskiĭ, J. Chem. Phys. **117**, 5940 (2002).
[49]M. Nakata *et al.*, Phys. Rev. A **18**, 2683 (1978).
[50]M. Nakata, N. Kuwahara, and M. Kaneko, J. Chem. Phys. **62**, 4278 (1975).
[51]J. Kojima, N. Kuwahara, and M. Kaneko, J. Chem. Phys. **63**, 333 (1975).
[52]A. Siporska, J. Szydlowski, and L. P. N. Rebelo, Phys. Chem. Chem. Phys. **5**, 2996 (2003).
[53]C. Ikier, H. Klein, and D. Woermann, Macromolecules **28**, 1003 (1995).
[54]C. C. Han and A. Ziya Akcasu, Polymer **22**, 1165 (1981).
[55]A. A. Silva, R. A. Reis, and M. L. L. Paredes, J. Chem. Eng. Data **54**, 2067 (2009).
[56]A. Negadi, M. Duval, and M. Benmouna, Polym. Bull. **43**, 261 (1999).